Current Biology 19, 2066–2076, December 29, 2009 ©2009 Elsevier Ltd All rights reserved DOI 10.1016/j.cub.2009.11.064

Article

A Broadly Conserved Pathway Generates 3′UTR-Directed Primary piRNAs

Nicolas Robine,[1,4] Nelson C. Lau,[2,4,5,*] Sudha Balla,[1,4] Zhigang Jin,[1] Katsutomo Okamura,[1] Satomi Kuramochi-Miyagawa,[3] Michael D. Blower,[2] and Eric C. Lai[1,*]

[1]Department of Developmental Biology, Sloan-Kettering Institute, 1275 York Ave, Box 252, New York, NY 10065, USA

[2]Department of Molecular Biology, Massachusetts General Hospital, 185 Cambridge Street, Boston, MA 02114, USA and Department of Genetics, Harvard Medical School, Boston, MA 02115, USA

[3]Department of Pathology, Medical School, Graduate School of Frontier Biosciences, Research Institute for Microbial Diseases, Osaka University, Yamada-oka 2-2 Suita, Osaka 565-0871, Japan

Summary

Background: Piwi-interacting RNAs (piRNAs) are ~24–30 nucleotide regulatory RNAs that are abundant in animal gonads and early embryos. The best-characterized piRNAs mediate a conserved pathway that restricts transposable elements, and these frequently engage a "ping-pong" amplification loop. Certain stages of mammalian testis also accumulate abundant piRNAs of unknown function, which derive from noncoding RNAs that are depleted in transposable element content and do not engage in ping-pong.

Results: We report that the 3′ untranslated regions (3′UTRs) of an extensive set of messenger RNAs (mRNAs) are processed into piRNAs in *Drosophila* ovaries, murine testes, and *Xenopus* eggs. Analysis of different mutants and Piwi-class immunoprecipitates indicates that their biogenesis depends on primary piRNA components, but not most ping-pong components. Several observations suggest that mRNAs are actively selected for piRNA production for regulatory purposes. First, genic piRNAs do not accumulate in proportion to the level of their host transcripts, and many highly expressed transcripts lack piRNAs. Second, piRNA-producing mRNAs in *Drosophila* and mouse are enriched for specific gene ontology categories distinct from those of simply abundant transcripts. Third, the protein output of *traffic jam*, whose 3′UTR generates abundant piRNAs, is increased in *piwi* mutant follicle clones.

Conclusions: We reveal a conserved primary piRNA pathway that selects and metabolizes the 3′UTRs of a broad set of cellular transcripts, probably for regulatory purposes. These findings strongly increase the breadth of Argonaute-mediated small RNA systems in metazoans.

Introduction

The Piwi family comprises a subclass of Argonaute proteins that are primarily expressed in invertebrate and vertebrate gonads and bind ~24–30 nucleotide RNAs termed Piwi-interacting RNAs (piRNAs) [1]. The best-studied function of the piRNA pathway is to maintain genomic integrity in the germline by restricting transposable element (TE) transcripts. Accordingly, most previously described *Drosophila* piRNAs derive from active TEs or from piRNA "master loci," which encode transcripts with substantial antisense TE sequences. These piRNAs fuel a cycle that selectively amplifies a posttranscriptional defense against active TEs, termed "piRNA ping-pong" [2, 3]. This pathway is ancient and deeply conserved among metazoans [4–6].

Much less is known about piRNAs that do not derive from TEs or other repetitive sequences. For example, intergenic noncoding transcripts that are relatively depleted in TEs generate extremely abundant piRNAs in mammalian pachytene testes [7–10]. The biogenesis and function of pachytene piRNAs are largely mysterious, and their lack of obvious antisense counterparts has made it difficult to infer their regulatory targets. It is presumed that pachytene piRNAs are made by a primary piRNA processing pathway that does not involve amplification.

We recently analyzed *Drosophila* OSS cells [11], a somatic ovarian cell line inferred to derive from a prefollicular cell progenitor [12]. In that study, we demonstrated that OSS cells express Piwi, but not Aub or AGO3, and consequently express only primary piRNAs [11]. This cell system is simplified relative to the intact gonad, which is composed of diverse cell types with varied expression of Piwi-class proteins. Although the majority of OSS cell piRNAs correspond to TEs and major piRNA clusters, we describe here a substantial population of piRNAs derived from protein-coding genes. Genic piRNAs preferentially arise from 3′ untranslated regions (3′UTRs) and are produced by a primary piRNA pathway that does not require ping-pong components. Large-scale piRNA sequencing in vertebrate cells reveals that the 3′UTR-directed piRNA pathway is conserved in vertebrates such as mice and *Xenopus*.

A shared feature of mRNA populations metabolized by this pathway in different species is that piRNA accumulation correlates only modestly with transcript abundance; a substantial proportion of highly expressed mRNAs do not generate piRNAs. This suggests that this pathway does not sample cellular transcripts indiscriminately. In support of this, gene ontology (GO) terms enriched among transcripts with abundant piRNAs were distinct from those of highly expressed mRNAs, and many GO terms were shared by piRNA-producing transcripts in fly and mouse gonads. In summary, we find that a substantial and conserved primary piRNA biogenesis pathway acts selectively on the 3′UTRs of messenger RNAs that function in gonadal and germline development.

Results

Distinct siRNA and piRNA Pathways Act upon 3′UTRs in *Drosophila* OSS Cells

We recently showed that the *Drosophila* OSS cell line generates abundant piRNAs and small interfering RNAs (siRNAs) from TEs [11]. Its accumulation of abundant piRNAs is shared

*Correspondence: nlau@brandeis.edu (N.C.L.), laie@mskcc.org (E.C.L.)
[4]These authors contributed equally to this work
[5]Present address: Department of Biology, Brandeis University, 415 South Street, Waltham, MA 02454, USA

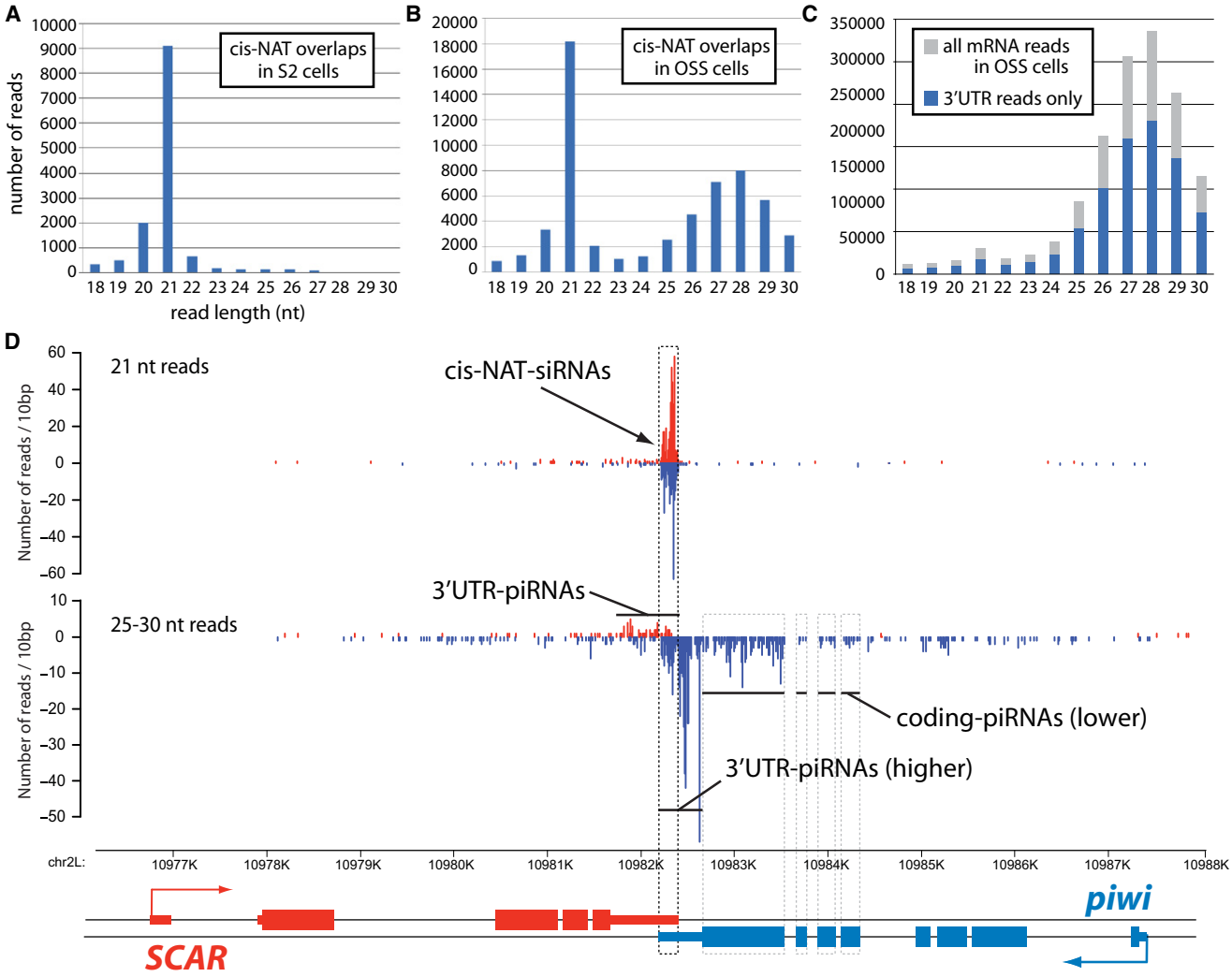

Figure 1. Distinct Spatial Patterns of siRNAs and piRNAs Mapped to mRNAs

(A) 3′ *cis*-natural antisense transcript (cis-NAT) overlap regions generate nearly exclusively 21 nt reads (siRNAs) in S2 cells.

(B) cis-NAT overlaps generate both siRNAs and piRNAs in OSS cells.

(C) Analysis of all mRNA-derived reads (blue) and 3′UTR reads (gray) from OSS cells shows that piRNAs are preferentially produced from 3′UTRs.

(D) Small RNAs produced by the *SCAR/piwi* cis-NAT in OSS cells. The complementary regions of the *SCAR/piwi* 3′UTRs specifically generate siRNAs; however, piRNAs are produced from along the length of the *SCAR* and *piwi* 3′UTRs. *piwi* coding exons also generate piRNAs, but fewer than does its 3′UTR.

only with gonadal tissues and early embryos [13–16]. On the other hand, diverse somatic and germline cells generate endo-siRNAs not only from TEs, but also from convergently transcribed protein-coding genes (3′ cis-NAT-siRNAs) [17–20]. Indeed, from 13.8 million mapped OSS small RNA reads, we categorized > 18,000 cis-NAT-siRNAs (Figure 1A and data not shown). Notably, *AGO2/CG7739* generated abundant siRNAs in both S2 cells (third highest in this cell type [17]) and in OSS cells (seventh highest in this cell type, 431 siRNAs mapped uniquely to the region of double-stranded transcription). Moreover, the third most highly expressed cis-NAT-siRNA locus in OSS cells was *piwi/SCAR* (Figure 1D, 699 siRNAs mapping uniquely to the overlap). Thus, transcripts for two Argonaute effectors are leading substrates of endo-RNAi in *Drosophila*.

Whereas the reads from S2 cell cis-NAT overlaps were strictly 21 nt in length, OSS cell cis-NAT overlap reads exhibited an unexpectedly bimodal size distribution reflecting both siRNAs and piRNAs (Figure 1B). The *piwi/SCAR* locus illustrated that piRNA production was not confined to the region of double-stranded transcription, as is characteristic of endo-siRNA production. Instead, piRNAs preferentially mapped to the sense strands of both *SCAR* and *piwi* 3′UTRs, and to a lesser extent from the *piwi* coding region. These patterns were representative of other cis-NATs in OSS cells and suggested that primary piRNAs derive from independent consumption of transcripts produced from either strand. The spatially segregated registers of piRNA and siRNA production within 3′UTRs indicated that, in addition to being translated, subpopulations of a transcript could enter multiple small RNA biogenesis pathways.

On the basis of these observations, we conducted a transcriptome-wide survey for piRNAs derived from annotated protein-coding transcripts, yielding 1.25 million such piRNAs (9.1% of all library reads, Figure 1C). Thus, the mRNA-directed primary piRNA pathway is highly active: the production of

3′UTR piRNAs is ~22% the amount of TE-piRNAs and ~30% the amount of microRNAs (miRNAs) in OSS cells [11]; mRNA-derived piRNAs outnumbered cis-NAT-siRNAs by 40-fold. This pathway is also broadly active: at an expression cutoff of > 50 piRNAs, we defined 2356 mRNAs that generated a total of 1.1 million piRNAs (see Table S1, available online). This compares with only 86 3′ cis-NAT pairs that generated > 50 siRNAs in the OSS data.

Over 70% (877,808) of mRNA-derived piRNAs mapped to 3′UTRs (Figure 1C), even though the aggregate length of 3′UTRs was much smaller than coding regions (5.4 Mb versus 22.5 Mb). The strong bias for 3′UTR-directed piRNA production was illustrated by plotting the cumulative relative density of piRNAs derived from 5′UTRs, CDS and 3′UTRs (Figure 2A). Despite this strong bias, a small subset of mRNAs preferentially generated piRNAs across their coding regions (Figure 2A).

The upper levels of piRNA accumulation were considerable: 180 genes generated > 1000 piRNAs (Table S1 and Figure S1). The loci with the most abundant 3′UTR piRNAs were *traffic jam* (*tj*) and *brain tumor* (*brat*) with > 67,000 and > 22,000 piRNAs, respectively; piRNAs covered the entirety of their 3′UTRs (Figures 2B and 2C). *tj* encodes a Maf-bZIP transcription factor expressed in somatic gonadal cells and required for ovary and testis development [21]. *brat* is a translational regulator required for development and growth control [22, 23] and has been implicated in the miRNA pathway [24]. The 3′UTR-directed piRNA pathway produced levels of small RNAs from some transcripts that were equivalent to reasonably highly expressed miRNAs (e.g., only 13 miRNA genes generated more reads than *tj*, Table S1).

Drosophila 3′UTR piRNAs Are Produced by a Primary Pathway Dependent on Piwi

To gain evidence for exonic piRNA production in the animal, we analyzed large-scale data of small RNAs from total ovaries and 0–2 hr embryos published by Hannon and colleagues [14]. We tallied ~100,000 such piRNAs in the combined available ovary data and ~65,000 piRNAs in the combined embryo data. When normalized for the total reads in each data set, OSS cells expressed considerably higher levels of 3′UTR-derived piRNAs, ~56,800 reads per million (RPM) versus 4,500 RPM in ovaries and 3,000 RPM in early embryos. We defined 316 and 253 transcripts in the ovary and embryo, respectively, that crossed a normalized threshold equivalent to the 50 piRNA cutoff for OSS cells. Importantly, the strong majority of 3′UTR piRNA-generating transcripts detected in the animal were shared by OSS cells (Figure S2A), indicating that this reflects a normal pathway rather than an aberrant feature of cultured OSS cells. The 12.6-fold elevation of 3′UTR-derived piRNAs in OSS cells was in line with our observation that follicle cell-specific *flamenco* piRNAs were ~8-fold higher in OSS than in total ovaries [11], suggesting that 3′UTR piRNAs are preferentially generated in follicle cells. Similar to primary TE-piRNAs, 3′UTR-derived piRNAs exhibited a 5′ U bias (66% of 3′UTR piRNAs), which is also consistent with their production by a primary piRNA pathway.

The Hannon and Zamore groups recently sequenced ovarian small RNAs from heterozygous or homozygous mutants of diverse piRNA factors [25, 26]. Hannon and colleagues observed that all piRNA pathway mutants exhibited decreased levels of TE-piRNAs, but that only *piwi*, *zucchini*, and *flamenco* specifically decreased levels of flamenco piRNAs [25]. These and other observations supported a model in which germline cells (but not follicle cells) engage in strong ping-pong amplification and in which *zucchini* and *piwi* are uniquely involved in a primary piRNA biogenesis pathway in somatic ovarian cells.

We collected the mRNA-derived reads from these data sets and observed that 3′UTR-derived piRNAs (and coding exonic piRNAs to a lesser degree) exhibited many similarities to TE-piRNAs. For example, *zucchini* and *piwi* mutants were strongly decreased for mRNA-derived piRNAs (Figure 2D), consistent with their role in primary TE-piRNA biogenesis. *flamenco* did not alter 3′UTR piRNA population, befitting its status as a piRNA substrate rather than a biogenesis component per se. In contrast, the ping-pong factors *armi*, *krimper*, *spn-E*, *squash*, and *vasa* exhibited increased proportions of 3′UTR piRNAs. Although these data indicate that these factors are not required to generate genic piRNAs, they do not necessarily limit their accumulation. The mutants with the strongest reduction in piRNAs from the ping-pong cluster 42AB—*armi*, *spn-E*, and *krimper* [25]—correspondingly exhibited the highest proportions of 3′UTR piRNAs (Figure 2D). We hypothesize that the absence of TE-piRNA amplification may incidentally lead to higher representation of 3′UTR piRNAs in the remaining sequenced small RNAs.

Examination of the other Piwi-class mutants, *aub* and *ago3*, was also informative [25, 26]. Whereas *ago3* mutants exhibited increased proportions of 3′UTR piRNAs, similar to most other ping-pong mutants, *aub* had fewer such piRNAs. This suggested that Aub received some 3′UTR piRNAs via a primary biogenesis pathway operative in the germline, consistent with the notion that Aub and Piwi load primary piRNAs whereas AGO3 mostly contains secondary piRNAs [2, 3]. Still, the *piwi* mutation clearly had greatest effect on 3′UTR piRNA accumulation. Indeed, *piwi* exhibited substantial haploinsufficiency, given that *piwi* heterozygotes accumulated far fewer 3′UTR piRNAs than did *aub* or *ago3* heterozygotes (Figure 2E). In summary, these analyses support the existence of a primary piRNA biogenesis pathway in vivo, with specificity toward the 3′UTRs of protein-coding transcripts and marked dependence on PIWI.

Conservation of 3′UTR-Directed piRNAs in Vertebrates

We next assessed whether the mRNA/3′UTR-directed piRNA pathway was apparent in mammalian gonads. The proportion of prepachytene spermatocytes in relation to other testicular cell types is highest at 10 dpp; subsequently, postpachytene spermatocytes and spermatids dominate in the testes [27, 28]. At 10 dpp, Mili appears to be the sole Piwi protein expressed, whereas the adult testis expresses both Mili and Miwi [29]. We therefore analyzed published 10 dpp data [29] and generated new small RNA data from 8 week adult testes. For consistency of downstream analysis, we reprocessed the published data from the raw files in parallel with our new data and mapped them with Bowtie [30].

Exonic piRNAs have been noted [4, 8, 10, 29, 31], but their regional preferences within protein-coding transcripts were not previously characterized. Examination of published lists of the top 200 fetal, 100 prepachytene, and 94 postpachytene clusters [4, 10, 32] indicated that many could be reclassified as 3′UTR-directed piRNA clusters (Table S2A). For example, clusters ranked #34 and #2 in fetal and 10 dpp testis, respectively, comprise piRNAs from the *ELK4* 3′UTR, and adult testis cluster ranked #49 represents the *CBL* 3′UTR. As was the case in *Drosophila* follicle cells, we observed substantial bias for 3′UTR-directed piRNA production in mouse testes (Figure 3B), although some transcripts exhibited CDS- or 5′UTR-enriched

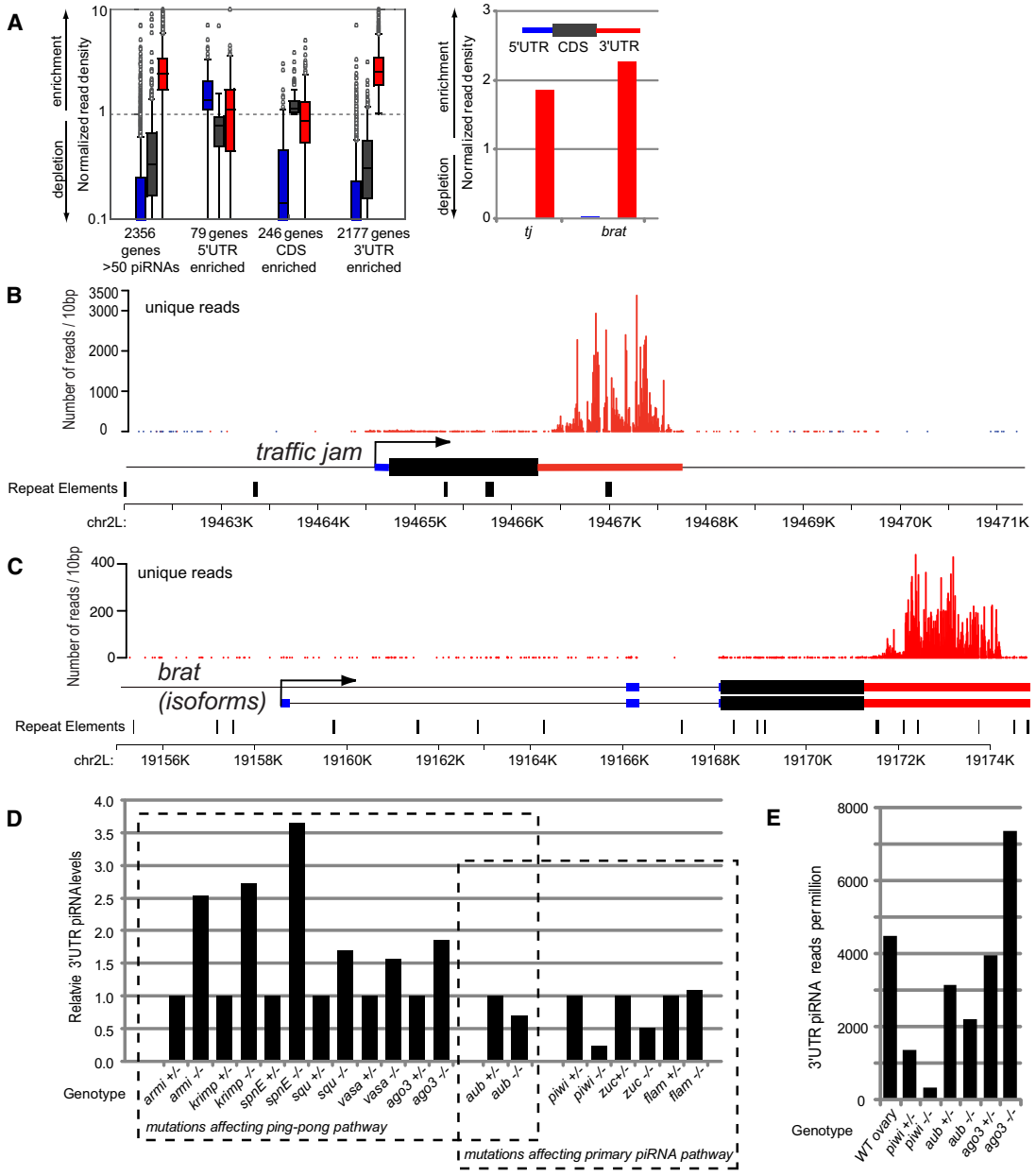

Figure 2. Preferred Production of piRNAs from 3′UTRs

(A) Normalized piRNA read density among the transcript features of 5′UTRs, CDS, and 3′UTRs in genes with > 50 piRNAs from OSS cells. Values greater than 1 indicate enrichment of piRNAs, values less than 1 indicate a depletion (see Supplemental Experimental Procedures). The box plot on the left shows the distribution of read density values among the group of genes with > 50 piRNAs and a breakdown of genes enriched in certain features. The boxes represent the upper and lower quartile, the line in each box indicates the median, the whiskers mark the minimum and maximum values in the range, and circles indicate outliers. The 3′UTR feature contains the majority of genes and the greatest overall enrichment values. The bar graph on the right shows the enrichment of piRNAs in the 3′UTR of *traffic jam* (*tj*) and *brat*. 5′UTR, CDS, and 3′UTR features are represented by blue, dark gray, and red colors, respectively.
(B and C) Example of 3′UTR-directed piRNA production from the *tj* and *brat* transcripts.
(D) Comparison of proportions of 3′UTR piRNAs in small RNA libraries from heterozygous and homozygous *Drosophila* mutants. 3′UTR levels in homozygotes were normalized to the levels in the corresponding heterozygotes.
(E) Normalized 3′UTR piRNA reads per million in wild-type and Piwi-class mutants. *piwi* heterozygous ovaries exhibit substantially lower 3′UTR piRNAs than to *aub* or *ago3* heterozygotes.

piRNAs. Overall, 3′UTR piRNAs were seemingly much more abundant at 10 dpp (~35% of all library reads) than in the adult (1.8% of all reads), although their representation in the adult library may incidentally be lowered because of the tremendous output of pachytene piRNA clusters (Table S2B) [7–10].

From combined data in 10 dpp and adult testes total RNA libraries, we identified 829 transcripts with 50 or more sense-oriented, uniquely mapping piRNAs, and 83 transcripts generated > 1000 piRNAs (Figure S3 and Tables S3A and S3B). For abundant piRNA-generating mRNAs, the strong majority of

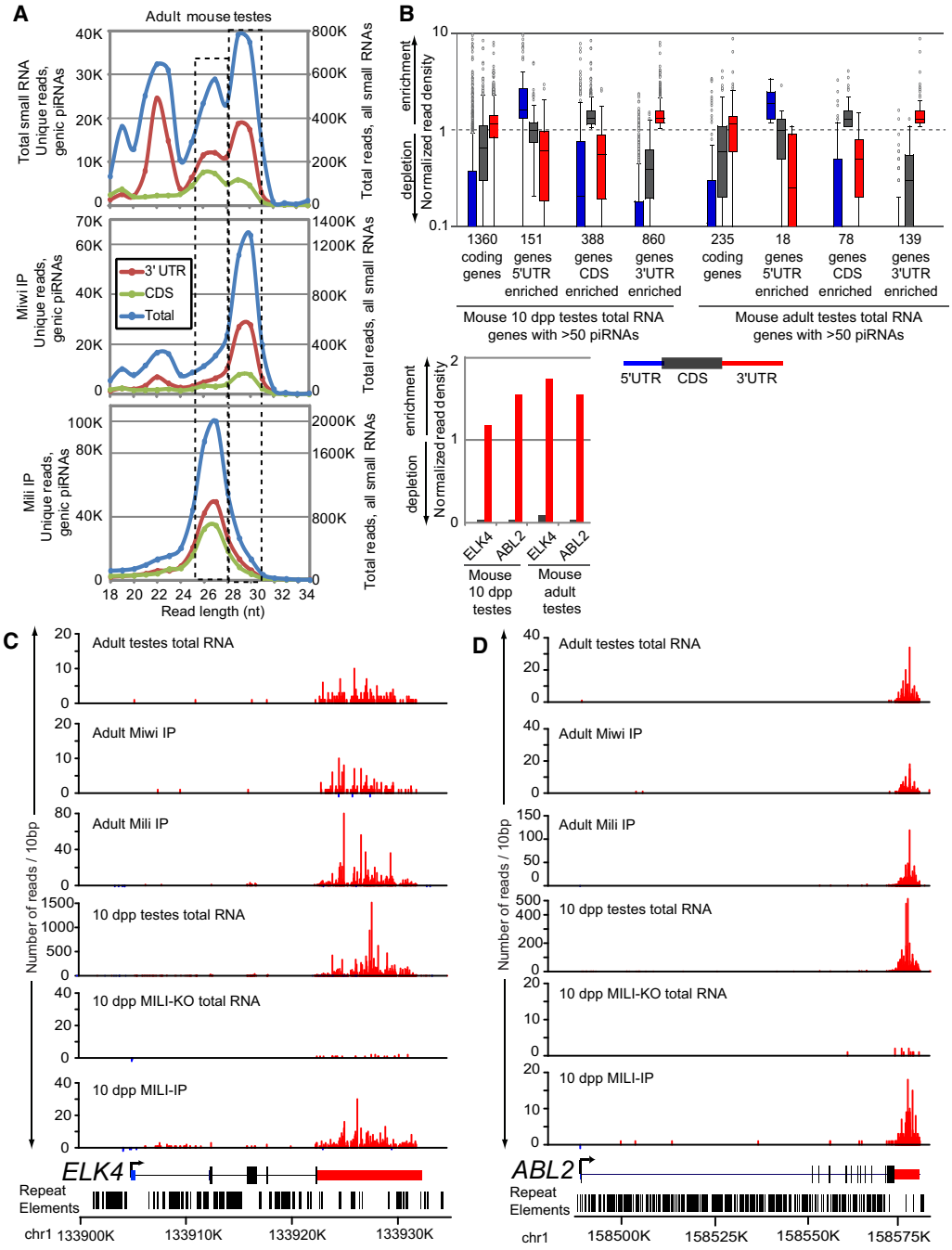

Figure 3. Mammalian 3′UTR-Directed piRNAs and Representative Directed Transcripts

(A) Size distribution of reads sequenced from total small RNAs (top graph), a MIWI IP (middle graph), and a MILI IP (bottom graph) from adult mouse testes extract. Dotted boxes highlight congruent peaks between the graphs.

(B) Normalized piRNA read density among the transcript features of 5′UTR, CDS, and 3′UTR in coding genes with > 50 piRNAs from mouse 10 dpp and adult testes. Values greater than 1 indicate enrichment of piRNAs; values less than 1 indicate a depletion (see Supplemental Experimental Procedures); and 5′UTR, CDS, and 3′UTR features are represented by blue, dark gray, and red colors, respectively. The box plot on the left shows the distribution of read density values among the group of coding genes with > 50 piRNAs and a breakdown of genes enriched in certain features. The boxes represent the upper and lower quartile, the line in each box indicates the median, the whiskers mark the minimum and maximum values in the range, and circles indicate outliers. In line with OSS cell genic piRNAs, the 3′UTR feature contains the majority of genes and the greatest overall enrichment values. The bar graph on the right shows the enrichment of piRNAs in the 3′UTR of *ELK4* and *ABL2*. Hundreds of murine transcripts, such as *ELK4* (C) and *ABL2* (D), preferentially generate piRNAs from the sense strand of their 3′UTRs (see also Figure S3). Repeats track indicates that 3′UTRs are strongly depleted in transposon/repetitive sequences.

piRNAs were located in 3′UTRs (424,227 uniquely mapping reads) relative to 5′UTR and CDS (55,799 total uniquely mapping reads). Even after normalization for gene lengths, piRNA density was highest among 3′UTRs in both 10 dpp and adult testes libraries (Figure 3B). The Ets-domain oncogene family gene, *ELK4*, and the Abelson murine leukemia viral

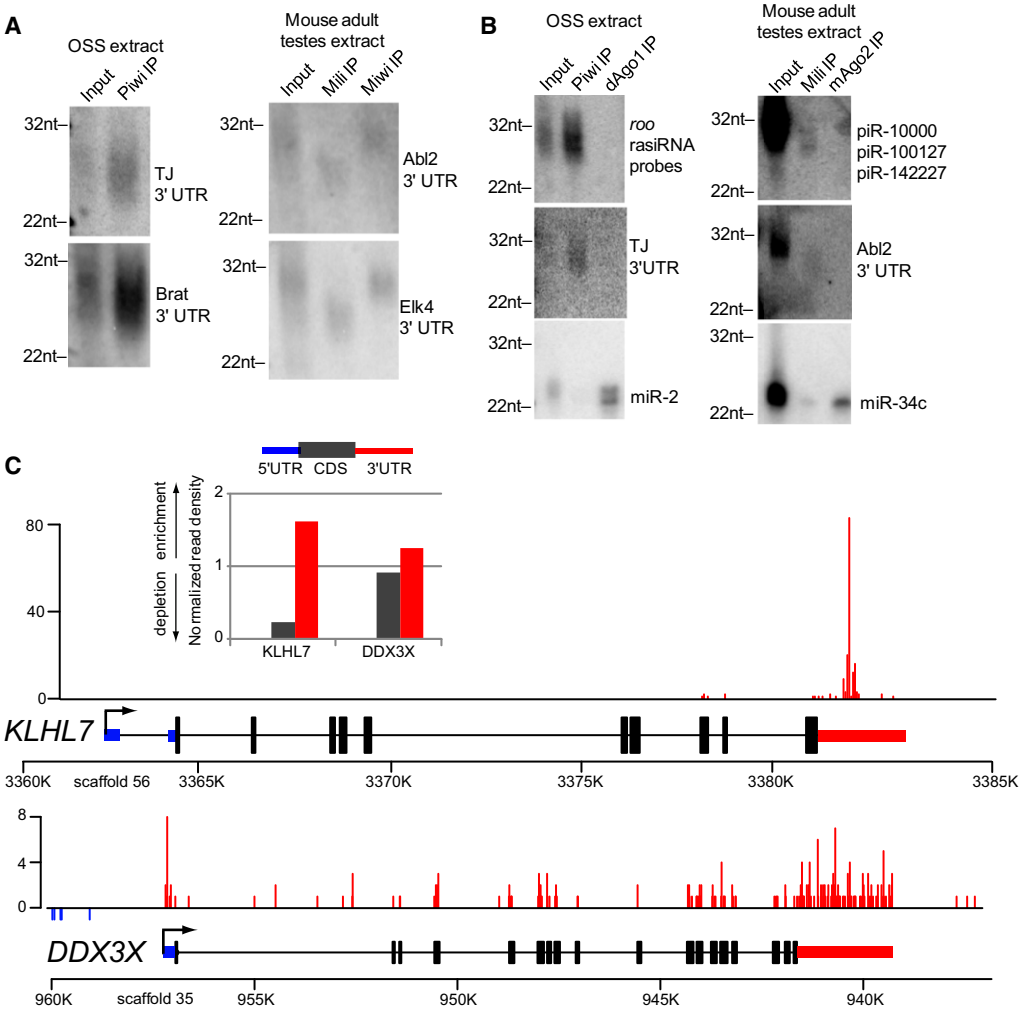

Figure 4. Association of 3′UTR-Directed piRNAs in Piwi-Protein Complexes

(A) RNAs from PIWI, MILI, and MIWI IPs were probed on northern blots with cloned 3′UTR fragments.

(B) The 3′UTR probes are specific for piRNAs from Piwi-protein IPs.

(C) Deep conservation of 3′UTR-directed piRNAs in animals. Enrichment of piRNA reads to the 3′UTR of *KLHL7* and *DDX3X* genes from an IP of *Xenopus* Piwi proteins with the Y12 antibody, as illustrated by the gene map and the bar graph of normalized piRNA read density according to transcript feature. 5′UTR, CDS, and 3′UTR features are represented by blue, dark gray, and red colors, respectively.

oncogene homolog 2, *ABL2*, serve as typical examples of transcripts with 3′UTR-directed piRNA production (Figures 3C–3D). The enrichment of 3′UTR piRNAs is actually more considerable because ~1/3 of the reads mapping outside of 3′UTRs derived from a few noncoding RNAs like *Rnu1b2*, *Snord22*, and *Gas5* (whose abundant reads came from point sources, Figure S4) or atypical genes like *Fth1* with abundant piRNA production from 5′UTR and CDS (Figure S5).

Analysis of a published 10 dpp library from *mili*$^{-/-}$ testes [29] revealed a strong depletion of genic piRNAs, including at 3′UTRs (Figure 3 and Figure S3). This genetic dependence echoed the observation that 3′UTR piRNAs are highly dependent on *Drosophila piwi*. Finally, we note a strong 5′ U bias (>85%) to murine mRNA/3′UTR-derived piRNAs, suggesting that these are primary piRNAs as in flies.

Loading of 3′UTR-Derived piRNAs into Piwi Complexes in Three Animal Clades

We next sought biochemical validation of the loading of 3′UTR piRNAs into Piwi complexes. Northern blots of Piwi immunoprecipitates (IPs) from OSS cells revealed that they carried piRNAs derived from the *tj* and *brat* 3′UTRs but did not contain the microRNA miR-2 (Figure 4). Reciprocally, AGO1-IP contained miR-2 but not 3′UTR piRNAs. In adult mouse testes, we detected *ABL2* and *ELK4* piRNAs in both Mili and Miwi complexes, but not in mAGO2 complexes. Equivalently sized probes directed at coding exons of these genes did not yield signal (data not shown), consistent with the much lower abundance of coding piRNAs from these mRNAs.

The peak size of 3′UTR piRNAs in Mili complexes (27–28 nt) was distinctly shorter than those in Miwi complexes (29–30 nt), reminiscent of the observation that different Piwi proteins associate with characteristic sizes of piRNAs [3, 29, 33]. The sizes of northern-blot signals from Miwi and Mili IPs were concordant with our deep-sequencing analysis (Figure 3A). However, the fact that bulk 3′UTR piRNAs in total RNA were the same size as those in Miwi-IP suggested that Miwi is the predominant carrier of 3′UTR piRNAs in adult testes. On the other hand, published 10 dpp Mili-IP data contained 3′UTR-biased distribution of 26–27 nt piRNAs, similar to total RNA

data from this stage [29]. Mili is believed to be the sole Piwi protein expressed at 10 dpp [4, 29], suggesting that Mili is the major carrier of 3′UTR piRNAs at this stage.

We confirmed the distribution of 3′UTR-derived piRNAs by sequencing 8.2 million Mili-IP- and 5.5 million Miwi-IP-mapped reads from adult testes and comparing these to our matched total RNA reads. To our knowledge, Mili-IP had not previously been deeply sequenced at this stage, and no deep Miwi-IP data have been reported thus far. Our total RNA library exhibited three size peaks at 22 nt, 27 nt, and 30 nt (Figure 3A); the former corresponds to miRNA reads whereas the latter two peaks correspond to piRNA reads. Consistent with the northern blots, these IP libraries showed that the larger peaks segregated precisely with the contents of Mili and Miwi complexes. In addition, the total RNA library exhibited greater representation of 3′UTR reads whose sizes corresponded to Miwi complexes, as we inferred from northern analysis. Nevertheless, the genes hit by piRNAs were relatively similar between Mili- and Miwi-IPs (data not shown), suggesting their production via a common primary pathway.

Finally, we assayed for 3′UTR piRNAs in Piwi complexes from an evolutionarily distant vertebrate outgroup species. We examined piRNAs from *Xenopus tropicalis* eggs that associated with the Y12 antibody, which binds symmetrically methylated arginines [34] that are present on diverse Piwi proteins [33, 35]. Despite incomplete genome annotation and the high proportion of reads from intergenic regions and TEs, we identified numerous annotated mRNAs with piRNAs corresponding to exons and 3′UTRs (Figure 4C, data not shown). These reads were less abundant than in mouse and *Drosophila*, but *KLHL7* and *DDX3X* serve as examples for piRNA enrichment at 3′UTRs. KLHL7 is implicated in ubiquitination and is associated with retinitis pigmentosa [36], and DDX3X is a helicase homologous to *Drosophila* Belle, which has been implicated as a component in the endo-RNAi pathway [37]. The existence of 3′UTR piRNAs in mature *Xenopus* germ cells provides evidence that this biogenesis pathway has been quite broadly conserved among animals.

Selective Production of 3′UTR-Directed piRNAs from Gonadal mRNAs

We next assayed the relationship of piRNA-producing transcripts with Affymetrix gene expression data from OSS cells (this study) and murine testis [38]. Comparing expression of mRNA generating 3′UTR piRNA with the general population, we observed that transcripts with moderate to high levels of piRNA were biased for higher expression (mean $\log_2$ expression = 6.7 for all transcripts called present, 7.3 for mRNAs with > 100 piRNAs, and 7.4 for mRNAs with > 1000 piRNAs, Figure S2B). Nevertheless, a large population of highly expressed transcripts (385 transcripts with $\log_2$ expression value of > 8) did not generate piRNAs, indicating that piRNA production was not strictly determined by transcript abundance. This was illustrated by plotting the gene expression of all mRNAs versus those that generated > 100 piRNAs and > 1000 piRNAs (Figure 5A). One might have expected transcripts with higher piRNA production to be greatly skewed toward higher expression levels; instead, the mRNAs with highest piRNA production spanned the full range of transcript accumulation.

The same was true for 10 dpp and adult mouse testes. Although there was a slight skew for piRNA-producing transcripts toward higher steady-state levels, they exhibited a similar distribution as the profile of all genes that are expressed in mouse testes (Figure 5A). These data suggest that the primary piRNA pathway selects the 3′UTRs of transcripts across a broad expression range, rather than acting nonspecifically on transcripts in proportion to their abundance.

Selection of Transcripts with Specific GO Enrichments by the Primary piRNA Pathway

Because there appeared to be selectivity for mRNA substrates by the primary piRNA pathway, we tested for enrichment of specific gene ontology (GO) categories. We first analyzed 646 OSS mRNAs that generated > 200 3′UTR piRNAs and had GO terms (regardless of gene expression level), relative to a background set of ~3000 lowly expressed OSS transcripts with GO terms. To assess whether piRNA-producing genes exhibited properties that were distinct from merely abundant transcripts, we analyzed the 675 most abundant OSS mRNAs that produced few (<10) piRNAs. These gene sets overlapped modestly in their GO terms, which included cytoskeleton, RNA, and protein metabolism processes (Figure 5B, Table S4). However, the themes among GO terms exclusively represented in either data set were notably different: abundant genes lacking piRNAs were most highly enriched in "housekeeping" GO categories such as general biosynthesis, metabolism, translation and ribosome components, and general transcription machinery. In contrast, the most highly enriched GO terms among genes with abundant 3′UTR piRNAs included categories such as development, morphogenesis, and regulatory processes, as well as DNA binding proteins, kinases, and phosphatases. The specific enrichment of many regulatory and developmental functions among abundant piRNA-generating genes, but not among abundantly expressed genes per se, suggested regulatory coherence by the primary piRNA pathway.

To analyze the murine data, we used cutoffs of $\geq$ 50 piRNAs/mRNA in 10 dpp total RNA library and $\geq$ 10 piRNAs/mRNA in total RNA, Mili-IP, and Miwi-IP in adult testis libraries (to account for lower 3′UTR piRNA content in adult libraries). Equivalently sized cohorts of mRNAs with high 3′UTR piRNAs and a nonoverlapping set of the highest expressed mRNAs without piRNAs revealed no overlap in enriched GO Function categories and only a modest overlap in Process categories (Figure 5C, Table S5), indicating that genes that generated abundant piRNAs were functionally distinct from abundant transcripts. Terms highly enriched in abundant transcripts lacking piRNAs at both 10 dpp and adult testes included many housekeeping categories, such as catabolism, translation, and ribosome components. On the other hand, terms that were highly and uniquely enriched among abundant piRNA transcripts included transcription and nucleic acid metabolic processes and zinc ion-binding and kinase-related functions.

Taken together, these analyses clearly demonstrate that abundant piRNA-producing transcripts in *Drosophila* OSS cell and murine testis comprise gene cohorts whose functions are very distinct from those of highly expressed transcripts in either species. Interestingly, several of the GO categories enriched in piRNA-producing transcripts were shared between fly and mouse gonads, even though the actual genes involved were quite different. We take this as a strong suggestion that the selection of mRNAs encoding certain types of GO functions is important to the operation of the 3′UTR-directed piRNA pathway. Interestingly, posttranscriptional gene silencing by RNA was a category enriched among abundant piRNA-generating mRNAs in both OSS cells and adult murine testes,

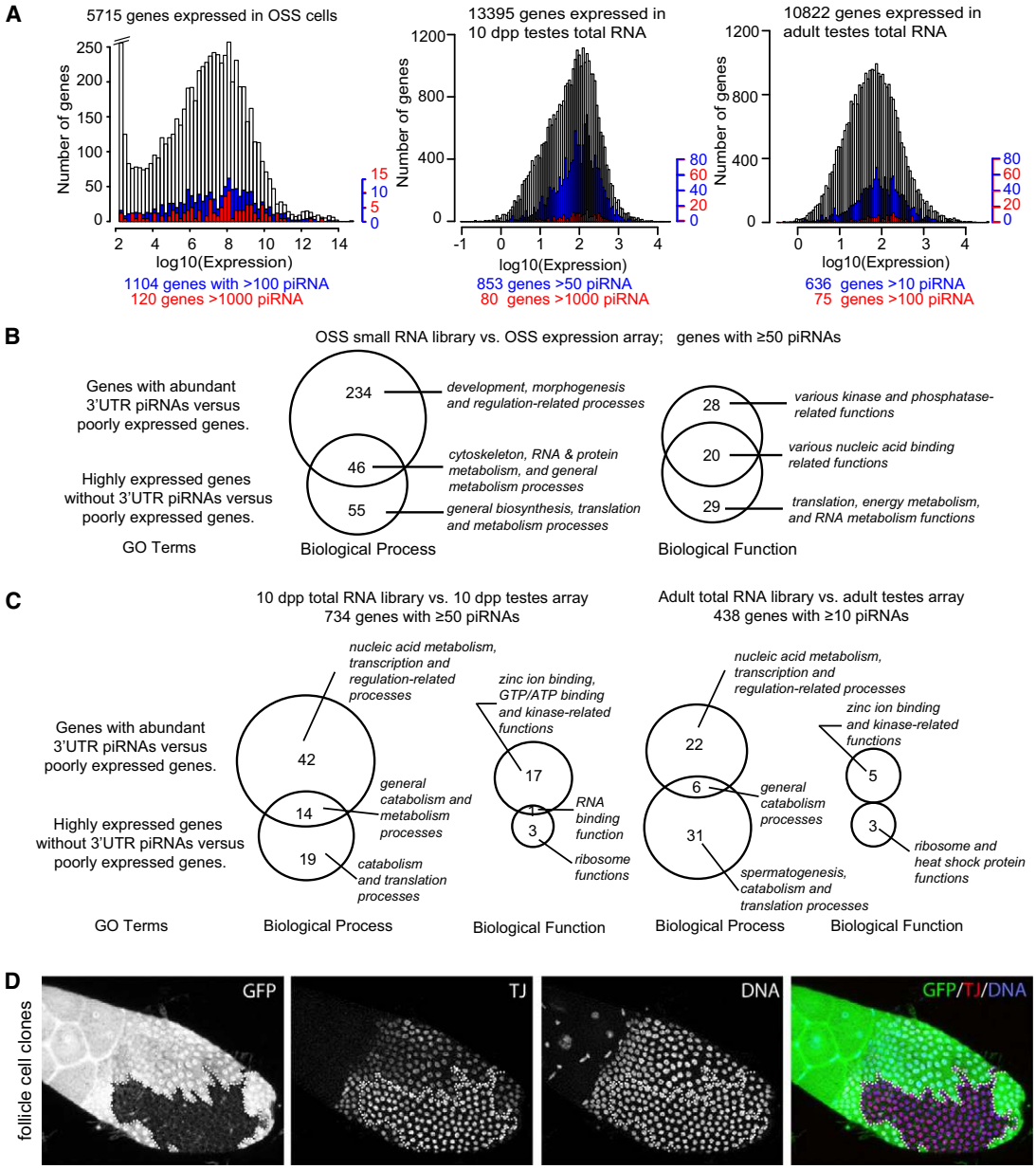

Figure 5. The mRNA/3′UTR piRNA Pathway Selects Certain Genes for Entry into the Pathway

(A) Histograms of genes by their ranked $\log_{10}$ expression levels and their corresponding count of 3′UTR piRNAs from OSS cells, mouse 10 dpp testes total RNA, and mouse adult testes total RNA libraries. Expressed genes are represented in white bars; genes with noted cutoff of piRNAs are in blue or red bars.

(B) Venn diagrams showing the comparison of GO term enrichments in mRNAs with abundant 3′UTR-directed piRNAs from OSS cells. Shown are counts of GO terms enriched among mRNAs with abundant (>1000 reads) and preferred production of piRNAs from 3′UTRs. Callout labels highlight notable GO terms with the strong statistical significance ($p < 10^{-4}$).

(C) Venn diagrams comparing GO term enrichments between mRNAs with abundant 3′UTR-directed piRAs and highly expressed mRNAs lacking 3′UTR piRNAs in mouse 10 dpp and adult testes. Details of the GO analyses, including of piRNA-producing transcripts lacking preferred 3′UTR enrichment, are available in Tables S4 (fly) and S5 (mouse).

(D) Staining of *piwi* mutant follicle clones with GFP antibody (green, to identify clone borders), TJ antibody (red), and DAPI (blue, to identify nuclei). Homozygous *piwi* mutant clones, as marked by absence of GFP, exhibit elevated levels of TJ.

but not among abundant transcripts in either tissue. In *Drosophila*, these genes included *brat*, *Dcr-2*, *RM62*, *AGO1 gawky/GW182*, and *piwi* (Table S1), whereas in mouse these included *TNRC6b*, *eif2c2/mAgo2*, *eif2c4/mAgo4*, and *piwil2/mili* (Tables S3A and S3B).

Beyond the small subset of small RNAs that coincidentally derive from cis-NATs or are related to TEs (e.g., Figures 1D and 3), the bulk of mRNA/3′UTR-derived piRNAs lack highly complementary sequences in the transcriptome (data not shown). Although some mRNA/3′UTR-derived piRNAs conceivably guide the regulation of *trans*-encoded targets bearing imperfect matches, a more proximal effect is the removal of 3′UTRs from transcripts via abundant piRNA production. However, we did not observe substantial, consistent changes

in the average expression of murine piRNA-producing mRNAs in *mili*$^{+/-}$ versus *mili*$^{-/-}$ testes (Table S6).

In principle, the results from whole gonads might be confounded if only a subset of cells have the capacity for piRNA generation and/or if there is a discrepancy between mRNA and protein output. We examined this in more detail by generating *piwi* mutant clones in *Drosophila* ovaries and staining them for TJ, whose mRNA generated the highest number of 3′UTR piRNAs in OSS cells. Although the penetrance was incomplete, we observed multiple cases in which TJ protein was upregulated in *piwi* mutant clones relative to neighboring control cells (Figure 5D). There appeared to be a temporal dependence in that younger clones did not exhibit increased levels of TJ, perhaps because of insufficient time for its deregulation. Nevertheless, these data support the notion that this pathway might influence target output.

Discussion

Genesis of Abundant Primary piRNAs from 3′UTRs in Diverse Animals

Our studies highlight the prevalence and conservation of mRNA substrates for the primary piRNA pathway and provide insight into primary piRNA biogenesis. Although clear orthologs between mouse and *Drosophila* Piwi proteins are not established, germline-associated cells in both systems engage a primary piRNA biogenesis pathway that preferentially generates abundant piRNAs from 3′UTRs. This class of piRNAs is especially abundant in *Drosophila* follicle cells (via Piwi) and in prepachytene-stage (via Mili) and pachytene-stage (via both Miwi and Mili) mammalian testes; we also detected a similar Aub-dependent pathway that probably operates in the *Drosophila* germline. While this work was under review, Siomi and colleagues also reported that a *piwi*- and *zucchini*-dependent primary piRNA pathway operates on the 3′UTRs of some *Drosophila* mRNAs [39]. Our conclusions on biogenesis are generally consistent. However, because our sequence data were ~1000 fold deeper, we could demonstrate that the primary piRNA pathway is not selective for a few mRNAs but instead acts broadly across > 1000 cellular transcripts and operates in both flies and vertebrates.

The mechanism of primary piRNA biogenesis remains largely mysterious. We believe that mRNA/3′UTR-directed piRNAs derive from a primary processing pathway, based on their 5′ U bias, their extraordinary abundance in *Drosophila* OSS cells (which lack ping-pong), and their genetic independence from ping-pong components in the animal. Previous studies noted that some 3′UTRs harbored TE sequences, suggesting a potential relationship to TE-piRNA production [4, 29]. However, we observed no overall enrichment for TEs in the 3′UTRs of piRNA-generating mRNAs (data not shown). Indeed, many *Drosophila* and mammalian 3′UTRs with highest piRNA production were strongly depleted for repeat elements relative to their introns (e.g., Figures 2 and 3), and most mRNA-derived piRNAs mapped uniquely. Moreover, the clearly distinct patterns of siRNA and piRNA biogenesis within cis-NAT-3′UTRs (Figure 1), along with the fact that most abundant piRNA-generating transcripts are not arranged in *cis*-NATs, suggest that the endo-siRNA and primary piRNA pathways act independently on cellular transcripts.

The production of piRNAs from spliced transcripts and preferentially from 3′UTRs suggests that they may be processed from cytoplasmic transcripts engaged with ribosomes. This scenario is consistent with the cosedimentation of Miwi and Mili with polysome fractions [9, 40]. We do not exclude the possibility of 3′UTR-specific isoforms that generate piRNAs, but we did not detect such transcripts from loci with highly abundant 3′UTR piRNAs (data not shown). Instead, we speculate that the abrupt reduction of piRNA production from adjacent coding exons may reflect competition between the translation machinery and primary piRNA biogenesis machinery. Although the status of most putative noncoding loci has not generally been examined experimentally, we observed that many of them exhibit distributive patterns across their exons (Figure S4). On the other hand, some protein-coding genes also generate substantial CDS-piRNAs (e.g., *piwi*, Figure 1). A careful comparison of mRNA partitioning between free and translating pools with their capacity for piRNA generation would be an informative test of the competition model.

The Tudor-domain containing gene TDRD-1 interacts with Miwi and Mili [33] and was suggested to regulate the formation of intergenic piRNAs versus genic piRNAs [31]. We confirmed that genic piRNAs derived predominantly from 3′UTR piRNAs were elevated in published 15 dpp *TDRD-1 KO* library comparable to 10 dpp wild-type libraries [31] (Table S2B). However, we did not observe a similarly high proportion of 3′UTR piRNAs in other published data from *TDRD-1* null 18.5 dpc testis (Tables S2B and S2C) [33]. We note that *TDRD-1* mutants exhibit apoptotic postpachytene spermatocytes at 15 dpp [41]. This probably reduces the contribution of postpachytene intergenic piRNAs, which may concomitantly increase the proportion of 3′UTR piRNAs in total small RNA libraries. This developmental defect provides an alternate basis besides a direct role for TDRD-1 in piRNA substrate selection [31].

The existence of abundant 3′UTR-derived piRNAs raises their potential relationship with pyknons [42]. Genic instances of pyknons are concentrated in 3′UTRs, and these transcripts are enriched for some GO terms that are shared by genes with abundant 3′UTR piRNAs (such as transcription and nucleic acid metabolism). However, 3′UTRs broadly produce piRNAs from across their lengths with little specificity for individual sequences, and pyknons do not exhibit preference for 5′ uridine as 3′UTR piRNAs do. In addition, although pyknons are defined as having multiple (>40) intergenic and genic instances [42], the vast majority of genic piRNAs map uniquely. These properties suggest that the primary piRNA pathway metabolizes 3′UTRs independently of pyknons.

Biological Function of the 3′UTR-Directed Primary piRNA Pathway

A challenge for the future is to understand the biological consequences of the 3′UTR-directed primary piRNA pathway. Given that piRNA-generating transcripts were not consistently altered in *mili-KO* mutants, it is prudent to consider that these piRNAs might be incidental, perhaps by-products of poised TE defense operation. On the other hand, it seems difficult to imagine that they entirely lack regulatory consequences given their sheer abundance: 3′UTR piRNAs comprise nearly 10% of small RNAs in *Drosophila* OSS cells and 35% of small RNAs in 10 dpp mouse testis.

Given the breadth of mRNA substrates, it is also conceivable that the primary piRNA pathway selects its substrates indiscriminately, perhaps in an attempt to identify selfish genetic material. However, this scenario is not reconciled with the observation that very substantial populations of abundant transcripts in *Drosophila* and mouse gonads do not generate 3′UTR piRNAs. Therefore, the piRNA pathway can no longer

be seen simply as having to choose between self (endogenous transcripts) and nonself (e.g., TEs). Instead, it must further route specific populations of host transcripts for 3′UTR-directed piRNA production, which we hypothesize has regulatory consequences.

Such regulation may operate in *cis* or in *trans*. In support of the former scenario, the *tj* 3′UTR is one of the most abundant sources of mRNA-derived piRNAs, and we observed increased levels of the TJ transcription factor in *piwi* mutant clones of appropriate age (Figure 5D). Perhaps more compelling was the finding that mRNAs selected for abundant 3′UTR piRNA production were enriched in a variety of GO categories that were not representative of abundant transcripts per se. We take this as an indication that these transcripts were actively selected for piRNA production. Moreover, the fact that many GO categories were shared by abundant piRNA-generating transcripts between *Drosophila* and mouse, such as kinase-related factors, DNA binding factors, and RNA silencing factors, suggests that they represent functionally conserved targets of the primary piRNA pathway.

It is also conceivable that mRNA/3′UTR-derived piRNAs serve as guides to regulate the expression of other transcripts. While this work was under review, Siomi and colleagues proposed that *tj*-derived 3′UTR piRNAs regulate cell adhesion genes such as *fas III*, potentially via partially complementary sequences within its ~60 kb intron [39]. Our data do not address this model; however, the candidate *fas III*-targeting *tj* piRNAs account for only 2.7% of *tj* piRNAs and only 0.15% of all 3′UTR piRNAs in our OSS data. Genetic modification of the *tj* 3′UTR in its endogenous context may clarify whether these particular *tj* piRNAs indeed serve critical *trans*-regulatory roles. Nevertheless, in light of the great abundance of mRNA/3′UTR piRNA complexes in *Drosophila* and mouse gonads, it is certainly plausible that they collectively have substantial *trans*-regulatory impact. In any case, the revelation of broad and abundant generation of piRNAs from cellular transcripts raises a new direction to understand how the piRNA pathway influences gonad and germ cell development.

Accession Numbers

The raw and processed mouse and *Xenopus* small RNA data reported herein are publicly available at the NCBI Gene Expression Omnibus under accession number GSE19172 and GSE19173, respectively.

Supplemental Data

Supplemental Data include detailed descriptions of small RNA library construction, bioinformatic procedures, molecular methods, and clonal analysis in the Supplemental Experimental Procedures, as well as five figures and six tables, and can be found with this article online at http://www.cell.com/current-biology/supplemental/S0960-9822(09)02118-6.

Acknowledgments

We thank Haruhiko and Mikiko Siomi for Piwi monoclonal antibody and open discussions. We are also grateful to Dorothea Godt for TJ antibody, to Haifan Lin for *piwi* stocks, to Kate Abruzzi and Michael Rosbash for reagents and assistance with Affymetrix gene profiling, and to Mark Borowsky and the MGH Illumina sequencing core for assistance in library sequencing. This work was partly supported by National Institutes of Health grant GM48405 to Robert Kingston and NIH grant GM086434 and a Career Award in the Biomedical Sciences from the Burroughs Wellcome Fund to M.D.B. Z.J. is a Research Fellow of The Terry Fox Foundation (#700132). K.O is supported by the Japan Society for the Promotion of Science. N.C.L. was funded by an NIH K99 grant (HD057298). Work in E.C.L.'s group was supported by the Kimmel Cancer Foundation, the Bressler Scholars Fund, and the NIH (R01-GM083300 and U01-HG004261).

Received: October 6, 2009
Revised: November 13, 2009
Accepted: November 25, 2009
Published online: December 17, 2009

References

1. Aravin, A.A., Hannon, G.J., and Brennecke, J. (2007). The Piwi-piRNA pathway provides an adaptive defense in the transposon arms race. Science *318*, 761–764.
2. Gunawardane, L.S., Saito, K., Nishida, K.M., Miyoshi, K., Kawamura, Y., Nagami, T., Siomi, H., and Siomi, M.C. (2007). A slicer-mediated mechanism for repeat-associated siRNA 5′ end formation in Drosophila. Science *315*, 1587–1590.
3. Brennecke, J., Aravin, A.A., Stark, A., Dus, M., Kellis, M., Sachidanandam, R., and Hannon, G.J. (2007). Discrete small RNA-generating loci as master regulators of transposon activity in Drosophila. Cell *128*, 1089–1103.
4. Aravin, A.A., Sachidanandam, R., Girard, A., Fejes-Toth, K., and Hannon, G.J. (2007). Developmentally regulated piRNA clusters implicate MILI in transposon control. Science *316*, 744–747.
5. Houwing, S., Kamminga, L.M., Berezikov, E., Cronembold, D., Girard, A., van den Elst, H., Filippov, D.V., Blaser, H., Raz, E., Moens, C.B., et al. (2007). A role for Piwi and piRNAs in germ cell maintenance and transposon silencing in Zebrafish. Cell *129*, 69–82.
6. Grimson, A., Srivastava, M., Fahey, B., Woodcroft, B.J., Chiang, H.R., King, N., Degnan, B.M., Rokhsar, D.S., and Bartel, D.P. (2008). Early origins and evolution of microRNAs and Piwi-interacting RNAs in animals. Nature *455*, 1193–1197.
7. Aravin, A., Gaidatzis, D., Pfeffer, S., Lagos-Quintana, M., Landgraf, P., Iovino, N., Morris, P., Brownstein, M.J., Kuramochi-Miyagawa, S., Nakano, T., et al. (2006). A novel class of small RNAs bind to MILI protein in mouse testes. Nature *442*, 203–207.
8. Girard, A., Sachidanandam, R., Hannon, G.J., and Carmell, M.A. (2006). A germline-specific class of small RNAs binds mammalian Piwi proteins. Nature *442*, 199–202.
9. Grivna, S.T., Pyhtila, B., and Lin, H. (2006). MIWI associates with translational machinery and PIWI-interacting RNAs (piRNAs) in regulating spermatogenesis. Proc. Natl. Acad. Sci. USA *103*, 13415–13420.
10. Lau, N.C., Seto, A.G., Kim, J., Kuramochi-Miyagawa, S., Nakano, T., Bartel, D.P., and Kingston, R.E. (2006). Characterization of the piRNA complex from rat testes. Science *313*, 363–367.
11. Lau, N.C., Robine, N., Martin, R., Chung, W.J., Niki, Y., Berezikov, E., and Lai, E.C. (2009). Abundant primary piRNAs, endo-siRNAs, and microRNAs in a Drosophila ovary cell line. Genome Res. *19*, 1776–1785.
12. Niki, Y., Yamaguchi, T., and Mahowald, A.P. (2006). Establishment of stable cell lines of Drosophila germ-line stem cells. Proc. Natl. Acad. Sci. USA *103*, 16325–16330.
13. Aravin, A.A., Lagos-Quintana, M., Yalcin, A., Zavolan, M., Marks, D., Snyder, B., Gaasterland, T., Meyer, J., and Tuschl, T. (2003). The small RNA profile during *Drosophila melanogaster* development. Dev. Cell *5*, 337–350.
14. Brennecke, J., Malone, C.D., Aravin, A.A., Sachidanandam, R., Stark, A., and Hannon, G.J. (2008). An epigenetic role for maternally inherited piRNAs in transposon silencing. Science *322*, 1387–1392.
15. Chung, W.J., Okamura, K., Martin, R., and Lai, E.C. (2008). Endogenous RNA interference provides a somatic defense against Drosophila transposons. Curr. Biol. *18*, 795–802.
16. Vagin, V.V., Sigova, A., Li, C., Seitz, H., Gvozdev, V., and Zamore, P.D. (2006). A distinct small RNA pathway silences selfish genetic elements in the germline. Science *313*, 320–324.
17. Okamura, K., Balla, S., Martin, R., Liu, N., and Lai, E.C. (2008). Two distinct mechanisms generate endogenous siRNAs from bidirectional transcription in Drosophila melanogaster. Nat. Struct. Mol. Biol. *15*, 581–590.
18. Ghildiyal, M., Seitz, H., Horwich, M.D., Li, C., Du, T., Lee, S., Xu, J., Kittler, E.L., Zapp, M.L., Weng, Z., and Zamore, P.D. (2008). Endogenous siRNAs derived from transposons and mRNAs in Drosophila somatic cells. Science *320*, 1077–1081.
19. Czech, B., Malone, C.D., Zhou, R., Stark, A., Schlingeheyde, C., Dus, M., Perrimon, N., Kellis, M., Wohlschlegel, J.A., Sachidanandam, R., et al.

(2008). An endogenous small interfering RNA pathway in Drosophila. Nature *453*, 798–802.

20. Kawamura, Y., Saito, K., Kin, T., Ono, Y., Asai, K., Sunohara, T., Okada, T.N., Siomi, M.C., and Siomi, H. (2008). Drosophila endogenous small RNAs bind to Argonaute 2 in somatic cells. Nature *453*, 793–797.
21. Li, M.A., Alls, J.D., Avancini, R.M., Koo, K., and Godt, D. (2003). The large Maf factor Traffic Jam controls gonad morphogenesis in Drosophila. Nat. Cell Biol. *5*, 994–1000.
22. Sonoda, J., and Wharton, R.P. (2001). Drosophila Brain Tumor is a translational repressor. Genes Dev. *15*, 762–773.
23. Frank, D.J., Edgar, B.A., and Roth, M.B. (2002). The Drosophila melanogaster gene brain tumor negatively regulates cell growth and ribosomal RNA synthesis. Development *129*, 399–407.
24. Neumüller, R.A., Betschinger, J., Fischer, A., Bushati, N., Poernbacher, I., Mechtler, K., Cohen, S.M., and Knoblich, J.A. (2008). Mei-P26 regulates microRNAs and cell growth in the Drosophila ovarian stem cell lineage. Nature *454*, 241–245.
25. Malone, C.D., Brennecke, J., Dus, M., Stark, A., McCombie, W.R., Sachidanandam, R., and Hannon, G.J. (2009). Specialized piRNA pathways act in germline and somatic tissues of the Drosophila ovary. Cell *137*, 522–535.
26. Li, C., Vagin, V.V., Lee, S., Xu, J., Ma, S., Xi, H., Seitz, H., Horwich, M.D., Syrzycka, M., Honda, B.M., et al. (2009). Collapse of germline piRNAs in the absence of Argonaute3 reveals somatic piRNAs in flies. Cell *137*, 509–521.
27. Bellvé, A.R., Cavicchia, J.C., Millette, C.F., O'Brien, D.A., Bhatnagar, Y.M., and Dym, M. (1977). Spermatogenic cells of the prepuberal mouse. Isolation and morphological characterization. J. Cell Biol. *74*, 68–85.
28. Nebel, B.R., Amarose, A.P., and Hacket, E.M. (1961). Calendar of gametogenic development in the prepuberal male mouse. Science *134*, 832–833.
29. Aravin, A.A., Sachidanandam, R., Bourc'his, D., Schaefer, C., Pezic, D., Toth, K.F., Bestor, T., and Hannon, G.J. (2008). A piRNA pathway primed by individual transposons is linked to de novo DNA methylation in mice. Mol. Cell *31*, 785–799.
30. Langmead, B., Trapnell, C., Pop, M., and Salzberg, S.L. (2009). Ultrafast and memory-efficient alignment of short DNA sequences to the human genome. Genome Biol. *10*, R25.
31. Reuter, M., Chuma, S., Tanaka, T., Franz, T., Stark, A., and Pillai, R.S. (2009). Loss of the Mili-interacting Tudor domain-containing protein-1 activates transposons and alters the Mili-associated small RNA profile. Nat. Struct. Mol. Biol. *16*, 639–646.
32. Kuramochi-Miyagawa, S., Watanabe, T., Gotoh, K., Totoki, Y., Toyoda, A., Ikawa, M., Asada, N., Kojima, K., Yamaguchi, Y., Ijiri, T.W., et al. (2008). DNA methylation of retrotransposon genes is regulated by Piwi family members MILI and MIWI2 in murine fetal testes. Genes Dev. *22*, 908–917.
33. Vagin, V.V., Wohlschlegel, J., Qu, J., Jonsson, Z., Huang, X., Chuma, S., Girard, A., Sachidanandam, R., Hannon, G.J., and Aravin, A.A. (2009). Proteomic analysis of murine Piwi proteins reveals a role for arginine methylation in specifying interaction with Tudor family members. Genes Dev. *23*, 1749–1762.
34. Lerner, E.A., Lerner, M.R., Janeway, C.A., Jr., and Steitz, J.A. (1981). Monoclonal antibodies to nucleic acid-containing cellular constituents: Probes for molecular biology and autoimmune disease. Proc. Natl. Acad. Sci. USA *78*, 2737–2741.
35. Kirino, Y., Kim, N., de Planell-Saguer, M., Khandros, E., Chiorean, S., Klein, P.S., Rigoutsos, I., Jongens, T.A., and Mourelatos, Z. (2009). Arginine methylation of Piwi proteins catalysed by dPRMT5 is required for Ago3 and Aub stability. Nat. Cell Biol. *11*, 652–658.
36. Friedman, J.S., Ray, J.W., Waseem, N., Johnson, K., Brooks, M.J., Hugosson, T., Breuer, D., Branham, K.E., Krauth, D.S., Bowne, S.J., et al. (2009). Mutations in a BTB-Kelch protein, KLHL7, cause autosomal-dominant retinitis pigmentosa. Am. J. Hum. Genet. *84*, 792–800.
37. Zhou, R., Hotta, I., Denli, A.M., Hong, P., Perrimon, N., and Hannon, G.J. (2008). Comparative analysis of argonaute-dependent small RNA pathways in Drosophila. Mol. Cell *32*, 592–599.
38. Shima, J.E., McLean, D.J., McCarrey, J.R., and Griswold, M.D. (2004). The murine testicular transcriptome: Characterizing gene expression in the testis during the progression of spermatogenesis. Biol. Reprod. *71*, 319–330.
39. Saito, K., Inagaki, S., Mituyama, T., Kawamura, Y., Ono, Y., Sakota, E., Kotani, H., Asai, K., Siomi, H., and Siomi, M.C. (2009). A regulatory circuit for piwi by the large Maf gene traffic jam in Drosophila. Nature *461*, 1296–1299.
40. Unhavaithaya, Y., Hao, Y., Beyret, E., Yin, H., Kuramochi-Miyagawa, S., Nakano, T., and Lin, H. (2009). MILI, a PIWI-interacting RNA-binding protein, is required for germ line stem cell self-renewal and appears to positively regulate translation. J. Biol. Chem. *284*, 6507–6519.
41. Chuma, S., Hosokawa, M., Kitamura, K., Kasai, S., Fujioka, M., Hiyoshi, M., Takamune, K., Noce, T., and Nakatsuji, N. (2006). Tdrd1/Mtr-1, a tudor-related gene, is essential for male germ-cell differentiation and nuage/germinal granule formation in mice. Proc. Natl. Acad. Sci. USA *103*, 15894–15899.
42. Rigoutsos, I., Huynh, T., Miranda, K., Tsirigos, A., McHardy, A., and Platt, D. (2006). Short blocks from the noncoding parts of the human genome have instances within nearly all known genes and relate to biological processes. Proc. Natl. Acad. Sci. USA *103*, 6605–6610.